Regular Paper (Cell)

Quantitative analysis of phagosome formation and maturation using an *Escherichia coli* probe expressing a tandem fluorescent protein

Maya Morita, Kazumasa Sawaki, Daiki Kinoshita, Chiye Sakurai, Naohiro Hori, and Kiyotaka Hatsuzawa*

Division of Molecular Biology, School of Life Sciences, Faculty of Medicine, Tottori University, Yonago, Tottori 683-8503, Japan

Running title: New *E. coli* probe for analysis of phagocytosis processes

Correspondence to: *Kiyotaka Hatsuzawa, Division of Molecular Biology, School of Life Sciences, Faculty of Medicine, Tottori University, Yonago, Tottori 683-8503, Japan. Tel: +81-859-38-6201, Fax: +81-859-38-6200, e-mail: hatsu@med.tottori-u.ac.jp

Abbreviations: DIC, differential interference contrast; DPI, diphenyleneiodonium; EGFP, enhanced green fluorescent protein; FBS, fetal bovine serum; FcR, Fcγ receptor; FITC, fluorescein isothiocyanate; GST, glutathione S-transferase; IPTG, isopropyl-β-D-1-thiogalactopyranoside; LC3, microtubule-associated protein 1 light chain 3; mCherry, monomeric Cherry; mRFP, monomeric red fluorescent protein; mVenus, monomeric Venus; NOX, NADPH oxidase; PBS, phosphate-buffered saline; PFA, paraformaldehyde; ROS, reactive oxygen species; SNAP-23, synaptosomal-associated protein of 23 kDa; SNARE, soluble *N*-ethylmaleimide-sensitive factor attachment protein receptor; TLR4, toll-like receptor 4; V-ATPase, vacuolar-type H+-ATPase.

Summary

Phagosome formation and maturation are essential innate immune mechanisms to engulf and digest foreign particles. To analyze these processes quantitatively, we established a specific *Escherichia coli* probe expressing a tandem fluorescent protein, comprising glutathione S-transferase fused with monomeric Cherry (mCherry) and monomeric Venus (mVenus). We demonstrated that mVenus was more susceptible to bleaching in an acidic environment than mCherry, and that the mVenus:mCherry fluorescence intensity ratio can be used to monitor phagosomal pH changes during maturation. Using this probe, we revealed that synaptosomal-associated protein of 23 kDa, a plasma membrane soluble *N*-ethylmaleimide-sensitive factor attachment protein receptor protein, actively regulated phagocytosis of *E. coli* and subsequent phagosome maturation in macrophages. Our results indicated that this probe has the potential to be a powerful tool in understanding the molecular mechanisms of phagosome formation and maturation.

***Keywords*:** *Escherichia coli*, macrophage, phagocytosis, phagosome maturation, tandem fluorescent protein

Phagocytosis is a form of endocytosis that is typically observed in phagocytes such as macrophages and dendritic cells. During phagocytosis, foreign particles larger than 0.5 μm, including many types of bacterial cells, yeast cells, and IgG-opsonized or complement-opsonized targets, are recognized by a specific cell surface receptor and then ingested by the cell. Binding of such a particle to a phagocytic receptor at the onset of phagocytosis activates a signaling cascade, which triggers actin cytoskeleton rearrangement and thus extensive plasma membrane deformation, ultimately leading to the formation of particle-containing phagosomes (*1, 2*). Newly formed phagosomes then gradually mature into phagolysosomes by sequentially fusing with endocytic compartments and lysosomes (*3, 4*). During this process, the microbicidal NADPH oxidase NOX2 is incorporated into early phagosomes, where it generates reactive oxygen species (ROS), whereas vacuolar-type H^+- ATPase (V-ATPase) recruited to the phagosome acidifies the phagosomal lumen, promoting lysosomal hydrolase activity (*5, 6*). Phagocytosis is therefore a vital process that allows the host immune system to defend against foreign particles (*1, 7*).

The fusion processes that occur during phagosome formation and maturation are regulated by several soluble *N*-ethylmaleimide-sensitive factor attachment proteins receptor (SNARE) proteins (*8–12*). We previously reported that synaptosomal-associated proteins of 23 kDa (SNAP-23), a plasma membrane-localized SNARE protein, plays a pivotal role in both phagosome formation and maturation during Fcγ receptor (FcR)-mediated phagocytosis in macrophages (*13*). When analyzing a macrophage line that stably overexpressed mVenus-tagged SNAP-23 (termed J774/mV-SNAP-23), we found that phagocytosis efficiency could not reliably be quantified using fluorescein isothiocyanate (FITC)-labeled zymosan particles opsonized with IgG. We showed that the efficiency of phagocytosis in J774/mV-SNAP-23 cells and control mVenus-expressing cells was similar using FITC-zymosan particles, but was enhanced in J774/mV-SNAP-23 cells when Texas Red-labeled zymosan particles were used (*13*). This most likely occurred, because the pH-sensitive fluorescent probe FITC is quenched in the acidic milieu of the phagosome during maturation, whereas red fluorescent probes such as Texas Red are more stable at low pH (*14*); however, the J774/mV-SNAP-23 cells ingested copious amounts of FITC-zymosan, and this promoted phagosomal acidification, which then reduced the fluorescence intensity, giving the appearance of phagocytosis efficiency similar to that of the control cells (*13*).

A stable particle probe that can be used to quantify the efficiency of phagosome formation and maturation over time to elucidate the molecular mechanisms of phagocytosis is clearly required. A particle conjugated with both pH-sensitive Oregon green 488 and pH-insensitive carboxytetramethylrhodamine is already available to monitor phagocytosis and phagosomal acidification (*15, 16*), but the labeling reagents for this type of probe are relatively costly and cannot be used with live bacteria. Furthermore, labeling of a particle with these reagents is very time consuming. An alternative approach using fluorescent proteins, including a

pH-sensitive green fluorescent protein (GFP), has been used in the biogenesis of lysosome-related organelles and autophagosomes. Monomeric red fluorescent protein (mRFP)-GFP-tagged LC3, an autophagosome marker, is widely used in the analysis of autophagosome maturation, as mRFP has a pKa of 4.5 and is therefore more resistant to acidic pH than GFP (*17, 18*). Other potentially useful fluorescent proteins include monomeric Venus (mVenus), derived from GFP, and monomeric Cherry (mCherry), derived from mRFP. Of these two, mVenus is more sensitive to phagosomal pH change (*19*).

In this study, we established and characterized an *Escherichia coli* probe expressing a GST-tagged Cherry (*E. coli*-mCherry) for the analysis of phagocytosis and an *Escherichia coli* probe expressing a GST-tagged mCherry-mVenus tandem fluorescent protein (*E. coli*-mCherry-mVenus) for the analysis of both phagosome formation and maturation. The activity of phagosomal hydrolases, and thus the efficiency of phagosome-lysosome fusion during the maturation process, was estimated using western blot analysis to assess the degradation of the *E. coli*-mCherry-mVenus probe. These probes are not only easy and inexpensive to produce, but also have the advantage of being able to simultaneously investigate the molecular mechanisms that regulate phagosome formation and maturation via receptors, such as toll-like receptor 4 (TLR4) and CD36 (*20–22*).

Materials and Methods

Materials

Isopropyl β-D-1-thiogalactopyranoside (IPTG) was purchased from Wako Pure Chemical Industries (Osaka, Japan). Diphenyleneiodonium chloride (DPI) was purchased from Enzo Life Science (Farmingdale, NY, USA). Bafilomycin A1 was purchased from Cayman Chemical (Ann Arbor, MI, USA). Polyclonal anti-GST-EGFP antibody was prepared as described previously (*11, 13, 23*), and anti-RFP antibody was a gift from Dr. Kenji Akasaki (Fukuyama University, Hiroshima, Japan) and Dr. Ikuo Wada (Fukushima Medical University, Fukushima, Japan) (*24*).

Cell Culture

J774 cells were obtained from the Riken Cell Bank (Tsukuba, Japan) and cultured in RPMI 1640 medium (Wako Pure Chemical Industries) supplemented with 10% fetal bovine serum (FBS) at 37°C in 5% CO_2. J774 cells stably expressing mVenus-tagged SNAP-23 were maintained in RPMI supplemented with 10% FBS and 2 μM puromycin to maintain selection (*13*).

Construction and expression of mCherry and mCherry-mVenus expression vectors

The plasmids pmVenus-C1 and pmCherry-C1 (Clontech-Takara Bio Inc., Shiga, Japan) were previously described (*11*). For construction of the pGEX-mCherry plasmid, PCR was used to generate mCherry cDNA with an exogenously added *Bam*HI restriction site at the 5′ end and removal of the initiation codon using the following primers: mChe-BamHI-Fw (5′-CGTGGATCCGTGAGCAAGGGCGAGG-3′) and Fluo-protein-Rv (5′-CCTCTACAAATGTGGTATGGC-3′). The PCR product was digested by *Bam*HI and *Eco*RI, and subcloned into the *Bam*HI-*Eco*RI site of the pGEX-4T-1 vector (GE Healthcare Bio-Sciences, Tokyo, Japan). To construct the vector encoding the tandem fluorescent protein, the PCR product from pmCherry-C1 was digested by *Bam*HI and *Kpn*I. mVenus cDNA was amplified from pmVenus-C1 to add a *Kpn*I restriction site at the 5′ end and remove its initiation codon using the following primers: mV-KpnI-Fw (5′-GACGGTACCGTGAGCAAGGGCGAGGAGCTG-3′) and Fluo-protein-Rv. Both the mCherry cDNA digested by *Bam*HI and *Kpn*I and the PCR product from pmVenus-C1 digested by *Kpn*I and *Eco*RI were subcloned into the *Bam*HI-*Eco*RI site of the pGEX-4T-1 vector to give the pGEX-mCherry-mVenus vector.

To express the GST-mCherry and GST-mCherry-mVenus fusion proteins, *E. coli* Rosetta (DE3)-competent cells (Novagen, Madison, WI, USA) were transformed with the pGEX-mCherry or pGEX-mCherry-mVenus vectors, respectively. Transformed Rosetta cells were cultured at 37°C in Luria-Bertani medium containing 100 μg/mL ampicillin until an OD_{600} of 0.6–0.8 units was reached, and then induced with 1 mM IPTG for 15 h according to manufacturer's protocol to give the probes termed *E. coli*-mCherry and *E. coli*-mCherry-mVenus. Cells were

harvested by centrifugation at 4500*g* for 20 min, washed three times in phosphate-buffered saline (PBS), and then fixed by gently rotating overnight at 4°C with 4% paraformaldehyde (PFA) in PBS.

Western blot analyses of* E.coli *probes expressing fluorescent proteins

To confirm the expression of the GST-fusion proteins at a small scale, the Rosetta cells transformed with the pGEX-mCherry and pGEX-mCherry-mVenus vectors were cultured for 2 h or 4 h at 37°C in the presence of 1 mM IPTG. Non-induced cells served as controls. Cells were then harvested by centrifugation at 4500*g* for 10 min and resuspended in sample buffer (20 mM Tris-HCl, pH 8.8, 1% SDS, 2 mM EDTA, 8% glycerol, 1% β-mercaptoethanol, and 0.01% bromophenol blue). SDS-PAGE and western blot were performed as described previously (*11, 13, 23*). Proteins were blotted onto Immobilon-P polyvinylidene difluoride membranes (Merck Millipore, Darmstadt, Germany) and probed with either anti-GST-EGFP or anti-RFP primary antibodies, followed by an horseradish peroxidase-conjugated anti-rabbit IgG secondary antibody. Proteins were then detected using ImmunoStar Zeta enhanced chemiluminescence reagent (Wako Pure Chemical Industries) and an ImageQuant LAS-4000 system (GE Healthcare Bio-Sciences) according to manufacturer's protocol.

To examine the effect of bafilomycin A1 on phagosomal degradation, J774 cells were incubated with *E. coli*-mCherry-mVenus probes in the presence or absence of bafilomycin A1 for 1 h at 37°C. Free probes were removed by washing with PBS, and then the cells were resuspended in sample buffer and whole-cell extracts were analyzed by SDS-PAGE and western blot, as described above. The density of a given band was quantified using ImageJ software (National Institutes of Health, Bethesda, MD, USA).

Validation of the pH sensitivity of* E. coli-*mCherry-mVenus probes

To increase the permeability of the bacterial cell membrane, E. coli-mCherry-mVenus probes were gently rotated in 0.2% Triton X-100 in PBS for 1 h at room temperature. Probes were then washed in PBS, resuspended in 25 mM Tris-HCl (pH 7.0–8.5), 25 mM sodium phosphate (pH 6.0–6.5), or 25 mM citric acid/sodium citrate (pH 4.0–5.5), and transferred to a 24-well plate at an OD_{600} of 2.5 units. The excitation and emission maxima of mVenus are 515 nm and 528 nm, respectively, whereas those of mCherry are 587 nm and 610 nm, respectively. Protein fluorescence was measured using an Infinite F500 microplate reader (TECAN, Kawasaki, Japan), with excitation and emission wavelengths of 485 nm and 535 nm, respectively, for mVenus, and excitation and emission wavelengths of 535 nm and 612 nm, respectively, for mCherry. The pH sensitivity of the *E. coli*-mCherry-mVenus probes was defined as the mVenus:mCherry fluorescence intensity ratio.

Phagocytosis assay using* E. coli *probes expressing fluorescent proteins

J774 cells or J774 cells stably expressing mVenus-tagged SNAP-23 were plated at 0.6×10^6 cells/well in a 24-well plate. Cells were then incubated for 1 h at 37°C, with or without permeabilized *E. coli*-mCherry or *E. coli*-mCherry-mVenus probes at an OD_{600} of approximately 2.5 units. Treated cells were washed with ice-cold PBS to remove the free probes and then incubated with 0.25 mg/mL Trypan blue in PBS to quench the fluorescence of any non-internalized probes prior to quantification of cellular fluorescence using an Infinite F500 microplate reader as described above. The cellular fluorescence, expressed as arbitrary fluorescence units, was defined as the fluorescence intensity observed in the presence of fluorescent probes minus that observed in the absence of the probe. The efficiency of phagocytosis was estimated from mCherry fluorescence intensity, and phagosome maturation efficiency was estimated from the mVenus:mCherry fluorescence intensity ratio.

Microscopy

J774 cells were incubated with the *E. coli* probes expressing fluorescent proteins at 37°C, washed with PBS, then fixed with 4% PFA in PBS for 30 min at room temperature. Images were captured on an LSM 780 meta laser-scanning microscope using 514 nm and 561 nm excitation and a Plan-Apochromat 63×/1.40 Oil DIC M27 objective lens (Carl-Zeiss, Oberkochen, Germany).

Statistics

Data are presented as the mean ± SE for the number of experiments indicated in figure legends. The statistical differences between the sample groups were analyzed with a two-tailed, paired Student's *t* test using GraphPad Prism software (GraphPad Software, San Diego, CA, USA). Statistical significance was defined as $p < 0.05$.

Results and Discussion

Creation of an E.coli *clone expressing the mCherry-mVenus tandem fluorescent protein*

The precise and quantitative analysis of both phagosome formation and maturation has led to significant advances in the understanding of innate immune responses and their molecular mechanisms. Several probes used in such analyses incorporate both fluorescent dyes and a fluorescent protein (*14–16, 25, 26*). *E.coli* particles, either labeled with FITC or expressing GFP, are occasionally used to quantify phagocytosis, but these fluorophores are likely to be quenched by the ROS and acidic pH that are generated within the formed phagosome during maturation (*25, 26*), resulting in imprecise quantification. Previous studies of phagosome maturation efficiency have used heat-killed bacteria co-labeled with both pH-sensitive and pH-insensitive chemical fluorophores (*15, 16*); however, such probes are relatively expensive and cannot be used to observe living bacteria.

We therefore attempted to establish an *E. coli* probe expressing either a single fluorescent protein and/or a tandem fluorescent protein. GST-mCherry and GST-mCherry-mVenus fusion proteins were created by cloning cDNAs encoding mCherry and mVenus into pGEX vector (Fig. 1A). *E. coli* gene expression was regulated using the lacIQ repressor and was induced with IPTG. The induction of protein expression was confirmed by western blot analysis using anti-GST-enhanced GFP (EGFP) antibodies (Fig. 1B). Before use, the *E. coli* probes were fixed with PFA/PBS to improve their stability, and permeabilized with Triton X-100/PBS such that their fluorescence could be easily quenched with Trypan blue when necessary (see *Materials and Methods* for details).

The *E. coli*-mCherry probe was efficiently ingested by murine macrophage-like J774 cells (Fig. 1C), with the phagocytosis efficiency of the probe increasing over time (Fig. 1D). A similar pattern was observed with the *E. coli*-mCherry-mVenus probe (data not shown). It is likely that phagocytosis of the pretreated *E. coli* probes is mediated by TLR4 and/or CD36, a class B scavenger receptor (*22*). As mCherry fluorescence is relatively insensitive to pH (*19*), the effect of phagosomal acidification was expected to be negligible, and the *E. coli*-mCherry probe signal within the phagosome can be used to accurately quantify the efficiency of phagocytosis (Fig. 1C and D). The *E. coli*-mCherry-mVenus tandem probe also incorporates the pH-sensitive mVenus protein. This tandem probe could therefore be used to simultaneously measure the efficiency of phagocytosis, via the mCherry fluorescence intensity, and the efficiency of phagosome maturation, via the mVenus:mCherry fluorescence intensity ratio.

The E. coli-*mCherry-mVenus probe can be used to detect changes in the acidic milieu of the phagosome*

To further investigate the fluorescent properties of the *E. coli*-mCherry-mVenus probe, we measured the mVenus:mCherry fluorescence intensity ratio in a buffer with a variable pH ranging from 4.0 to 8.5. We found that the mVenus:mCherry ratio gradually decreased in a pH-dependent manner (Fig. 2A), which was consistent with previous reports that mVenus fluorescence is more sensitive to pH than mCherry fluorescence (*19*). This suggested that the *E. coli*-mCherry-mVenus probe could be useful for analyzing the phagosomal environment. Next, J774 cells were incubated with this probe for 1 h, washed to remove unbound extracellular probes, and further incubated in probe-free medium. The mVenus:mCherry ratio was then measured at various time points up to 120 min (Fig. 2B). The intracellular mVenus:mCherry fluorescence intensity ratio decreased gradually over the measured time period, suggesting that the phagosome environment acquired the acidic milieu indicative of the maturation process.

These results were confirmed by confocal microscopic analysis of J774 cells after probe ingestion. Cells were incubated with the probe for 30 min, quickly washed to remove the unbound probes, and then incubated for up to 150 min as the phagosomes matured. Progressive bleaching of the mVenus signal was observed in the cells over time (Fig. 2C). Conversely, the mCherry signal was barely affected by the changes in phagosomal environment (Fig. 2C), as was seen with the *E. coli*-mCherry probe (Fig. 1C). The phagosomes containing the *E. coli*-mCherry-mVenus probe became smaller and increasingly fuzzy over time (Fig.2C), suggesting some degradation of the probe through the activity of phagosomal hydrolases.

Reduction in mVenus:mCherry fluorescence intensity ratio results from vacuolar H^+-ATPase activity

A reduction in the mVenus:mCherry fluorescence intensity ratio was observed during phagosome maturation, possibly because of vacuolar-type H^+-ATPase (V-ATPase) activity leading to the progressive acidification of the environment within macrophages. To investigate this hypothesis, we examined the effect of the specific V-ATPase inhibitor bafilomycin A1 on the intraphagosomal mVenus:mCherry ratio. Interestingly, application of bafilomycin A1 at concentrations higher than 10 nM led to an approximately 3-fold enhancement of the mVenus:mCherry fluorescence intensity ratio compared with the untreated control (0 nM inhibitor; Fig. 3A). The *E. coli*-mCherry-mVenus probe demonstrated no loss of mCherry signal over the measured bafilomycin A1 concentration range (Fig. 3B), suggesting that the increased ratio resulted from an attenuation of mVenus signal loss after treatment. Indeed, confocal microscopic analysis confirmed that there was no significant bleaching of the mVenus or mCherry signals in bafilomycin A1-treated cells compared with untreated controls (Fig. 3C).

ROS such as the hypochlorous acid (HOCl) that is generated within phagosomes by

activated NADPH oxidase complexes have been shown to bleach GFP fluorescence in neutrophils (*25*). We therefore examined the effect of NADPH oxidase activity on the mVenus:mCherry fluorescence intensity ratio using the potent flavoenzyme inhibitor DPI. Although the effect was less striking than that observed with bafilomycin A1, treatment of J774 cells with DPI resulted in an approximately 1.5-fold increase in mVenus:mCherry ratio within the phagosome, indicating a 1.5-fold reduction in mVenus signal suppression (Fig. 3A). Taken together, these results suggested that the *E. coli*-mCherry-mVenus probe was sensitive primarily to the V-ATPase-induced decrease in phagosomal pH that occurs within macrophages.

Western blot analysis of GST-mCherry-mVenus degradation products, detected using anti-RFP antibodies, revealed an inverse correlation between bafilomycin A1-induced V-ATPase inhibition and probe degradation, suggesting the concomitant occurrence of phagosomal hydrolase activity and acidification (Fig. 3D). The *E. coli* expressing GST-mCherry-mVenus was fixed with 4%PFA/PBS before use, and the resulting crosslinked products are shown in Fig. 3D as broad, high-molecular-weight bands. The major degradation product was approximately 28 kDa in size, which is consistent with the predicted molecular weight of mCherry, suggesting that this protein was cleaved from the probe as a single molecule. The possible persistence of dissociated, but intact, mCherry within the phagosome might partially explain the relative stability of the observed mCherry signal. Hydrolases are derived from lysosomes; degradation analysis could therefore be used to estimate the efficiency of phagosome-lysosome fusion within macrophages. The use of live, un-fixed *E. coli*-mCherry-mVenus probes for such analysis could lead to the more accurate and sensitive detection of degradation products.

In this analysis, the mVenus domain was not detected using anti-EGFP antibodies (data not shown) likely due to its complete digestion by lysosomal hydrolases (*27*), suggesting that effects from possible intramolecular Förster resonance energy transfer (FRET) caused in the probe upon phagosome maturation analysis were negligible. If the mVenus domain of the probe could be cleaved in its intact form within phagosomes, mVenus (donor) fluorescence would be enhanced by dissociation from the mCherry domain (acceptor). However, the mVenus fragment is unlikely intact during phagosome maturation due to the reason described above.

J774 cells overexpressing mVenus-SNAP-23 display enhanced E. coli *phagosome formation and maturation*

SNAP-23 is a plasma membrane-localized SNARE protein that participates in membrane fusion during exocytosis of several cell types (*12, 28*). Previously, we reported that in macrophages, SNAP-23 regulates the formation and maturation of phagosomes during FcR-mediated phagocytosis (*13*); however, the role of SNAP-23 in other types of receptor-mediated

phagocytosis remains unclear. J774 cells provide an opportunity to investigate this, as phagocytosis in these cells is mediated by receptors such as TLR4 and CD36 that are responsible for internalization of *E. coli* (*22*). We therefore used the *E. coli*-mCherry-mVenus probe to examine the efficiency of phagosome formation and maturation in J774 cells expressing mVenus-tagged SNAP-23 (J774/mVenus-SNAP-23). The expression of mVenus-SNAP-23 in these cells was previously confirmed at nearly twice that of endogenous SNAP-23 (*13*).

Compared with control cells expressing mVenus, J774/mVenus-SNAP-23 cells exhibited both significantly enhanced phagocytosis efficiency, estimated from the mCherry signal (Fig. 4A, right panel), and significantly enhanced phagosome maturation efficiency, estimated from the mVenus:mCherry fluorescence intensity ratio (Fig. 4B). The probe associated with both cell types with equal efficiency (Fig. 4A, left panel), confirming that these observations were not artifacts. The enhanced phagosome maturation efficiency observed in J774/mVenus-SNAP-23 cells was confirmed by western blot analysis of *E. coli*-mCherry-mVenus probe degradation (Fig. 4C). In this experiment, cells were incubated with the probe for 1 h in the presence or absence of 10 nM bafilomycin A1, before the free probe was removed and cells were incubated for an additional hour in probe-free medium. The amount of the 28 kDa degradation product at time 0, when the unbound probe was removed, was taken to be 1.0, and the level of observed degradation after an hour was normalized to this value. In the absence of bafilomycin A1, the increase in the 28 kDa degradation product in the hour after removal of unbound probe was more striking in J774/mVenus-SNAP-23 cells (11.86-fold) than in J774/mVenus cells (7.89-fold) (Fig. 4C). Taken together, these results suggested that SNAP-23 actively regulated membrane fusion events during TLR4- and/or CD36-mediated phagocytosis of *E. coli*, in a manner similar to FcR-mediated phagocytosis in macrophages reported previously (*13, 20–22*). Furthermore, our results showed that the *E. coli*-mCherry-mVenus probe was useful for the simultaneous investigation of the efficiencies of multiple processes. Future experiments using this probe might shed light on the mechanism of SNAP-23-mediated phagosome maturation that allows the efficient lipopolysaccharide (LPS)-stimulated cross-presentation of antigens downstream of TLR signaling (*29*).

Thus, we have developed a simple and inexpensive method for the simultaneous investigation of phagosome formation and maturation efficiencies, which will streamline the characterization of *E.coli* uptake, phagosomal acidification, and phagosome-lysosome fusion in macrophages over time. For this method, we have created an *E. coli* probe expressing a GST-tagged tandem fluorescent protein, composed of the pH-stable mCherry and the pH-sensitive mVenus proteins, termed *E. coli*-mCherry-mVenus. Using the stable fluorescence of mCherry and the mVenus:mCherry fluorescence intensity ratio, it is possible to use this probe to monitor both phagocytosis efficiency and the pH change associated with phagosomal acidification in

macrophages, respectively. Following ingestion of the *E. coli*-mCherry-mVenus probe, the activity of lysosomal acid hydrolases within phagosomes and, thus, phagosome-lysosome fusion efficiency can be investigated by detecting probe degradation products by western blot. Furthermore, the probe opsonized with anti-*E. coli* antibodies or GST-mCherry-mVenus-conjugated microbeads, which are opsonized with anti-GST-EGFP antibodies, can be used to investigate FcR-mediated phagocytosis. Overall, we believe that this method is useful for the analysis of the molecular mechanisms that regulate phagosome formation and maturation in phagocytes such as macrophages.

Funding

This work was supported in part by a Grant-in-Aid for Young Scientists (B) (#25860218) to C.S. from the Japan Society for the Promotion of Science, and C.S. was supported by the Takeda Science Foundation.

Acknowledgments

We are grateful to Ikuo Wada (Fukushima Medical University) for the gift of the anti-RFP antibody, as well as for helpful discussions and critical reading of the manuscript. We would like to thank Editage (www.editage.jp) for their help with English language editing.

Conflicts of Interest

None declared.

References

1. Desjardins, M., Houde, M., and Gagnon, E. (2005) Phagocytosis: the convoluted way from nutrition to adaptive immunity. *Immunol. Rev.* **207**, 158–165
2. Swanson, J.A. (2008) Shaping cups into phagosomes and macropinosomes. *Nat. Rev. Mol. Cell Biol.* **9**, 639–649
3. Vieira, O.V., Botelho, R.J., and Grinstein, S. (2002) Phagosome maturation: aging gracefully. *Biochem. J.* **366**, 689–704
4. Levin, R., Grinstein, S., and Canton, J. (2016) The life cycle of phagosomes: formation, maturation, and resolution. *Immunol. Rev.* **273**, 156–179
5. Nunes, P., Demaurex, N., and Dinauer, M.C. (2013) Regulation of the NADPH oxidase and associated ion fluxes during phagocytosis. *Traffic* **14**, 1118–1131
6. Canton, J. (2014) Phagosome maturation in polarized macrophages. *J. Leukoc. Biol.* **96**, 729–738
7. Kagan, J.C. and Iwasaki, A. (2012) Phagosome as the organelle linking innate and adaptive immunity. *Traffic* **13**, 1053–1061
8. Braun, V., Fraisier, V., Raposo, G., Hurbain, I., Sibarita, J.B., Chavrier, P., Galli, T., and Niedergang, F. (2004) TI-VAMP/VAMP7 is required for optimal phagocytosis of opsonized particles in macrophages. *EMBO J.* **23**, 4166–4176
9. Collins, R.F., Schreiber, A.D., Grinstein, S., and Trimble, W.S. (2002) Syntaxins 13 and 7 function at distinct steps during phagocytosis. *J. Immunol.* **169**, 3250–3256.
10. Murray, R.Z., Kay, J.G., Sangermani, D.G. and Stow, J.L. (2005) A role for the phagosome in cytokine secretion. *Science* **310**, 1492–1495
11. Hatsuzawa, K., Tamura, T., Hashimoto, H., Yokoya, S., Miura, M., Nagaya, H., and Wada, I. (2006) Involvement of syntaxin 18, an endoplasmic reticulum (ER)-localized SNARE protein, in ER-mediated phagocytosis. *Mol. Biol. Cell* **17**, 3964–3977
12. Stow, J.L., Manderson, A.P., and Murray, R.Z. (2006) SNAREing immunity: the role of SNAREs in the immune system. *Nat. Rev. Immunol.* **6**, 919–929
13. Sakurai, C., Hashimoto, H., Nakanishi, H., Arai, S., Wada, Y., Sun-Wada, G.H., Wada, I., and Hatsuzawa, K. (2012) SNAP-23 regulates phagosome formation and maturation in macrophages. *Mol. Biol. Cell* **23**, 4849–4863
14. Ip, W.K., Sokolovska, A., Charriere, G. M., Boyer, L., Dejardin, S., Cappillino, M. P., Yantosca, L. M., Takahashi, K., Moore, K. J., Lacy-Hulbert, A., and Stuart, L. M. (2011) Phagocytosis and phagosome acidification are required for pathogen processing and MyD88-dependent responses to *Staphylococcus aureus*. *J. Immunol.* **184**, 7071–7081
15. Vergne, I., Constant, P., and Laneelle, G. (1998) Phagosomal pH determination by dual fluorescence flow cytometry. *Anal. Biochem.* **255**, 127–132.

16. Akbar, M.A., Tracy, C., Kahr, W.H., and Kramer, H. (2011) The full-of-bacteria gene is required for phagosome maturation during immune defense in *Drosophila*. *J. Cell Biol.* **192**, 383–390
17. Kimura, S., Noda, T., and Yoshimori, T. (2007) Dissection of the autophagosome maturation process by a novel reporter protein, tandem fluorescent-tagged LC3. *Autophagy* **3**, 452–460
18. Fujiwara, E., Washi, Y., and Matsuzawa, T. (2013) Observation of autophagosome maturation in the interferon-gamma-primed and lipopolysaccharide-activated macrophages using a tandem fluorescent tagged LC3. *J. Immunol. Methods* **394**, 100–106
19. Doherty, G.P., Bailey, K., and Lewis, P.J. (2010) Stage-specific fluorescence intensity of GFP and mCherry during sporulation in *Bacillus Subtilis*. *BMC Res. Notes* **3**, 303
20. Kong, L. and Ge, B.X. (2008) MyD88-independent activation of a novel actin-Cdc42/Rac pathway is required for Toll-like receptor-stimulated phagocytosis. *Cell Res.* **18**, 745–755
21. Chen, Y.J., Hsieh, M.Y., Chang, M.Y., Chen, H.C., Jan, M.S., Maa, M.C., and Leu, T.H. (2012) Eps8 protein facilitates phagocytosis by increasing TLR4-MyD88 protein interaction in lipopolysaccharide-stimulated macrophages. *J. Biol. Chem.* **287**, 18806–18819
22. Cao, D., Luo, J., Chen, D., Xu, H., Shi, H., Jing, X., and Zang, W. (2016) CD36 regulates lipopolysaccharide-induced signaling pathways and mediates the internalization of *Escherichia coli* in cooperation with TLR4 in goat mammary gland epithelial cells. *Sci. Rep.* **6**, 23132
23. Hatsuzawa, K., Hashimoto, H., Arai, S., Tamura, T., Higa-Nishiyama, A., and Wada, I. (2009) Sec22b is a negative regulator of phagocytosis in macrophages. *Mol. Biol. Cell* **20**, 4435–4443
24. Suzuki, T., Arai, S., Takeuchi, M., Sakurai, C., Ebana, H., Higashi, T., Hashimoto, H., Hatsuzawa, K., and Wada, I. (2012) Development of cysteine-free fluorescent proteins for the oxidative environment. *PLoS One* **7**, e37551
25. Schwartz, J., Leidal, K.G., Femling, J.K., Weiss, J.P., and Nauseef, W.M. (2009) Neutrophil bleaching of GFP-expressing staphylococci: probing the intraphagosomal fate of individual bacteria. *J. Immunol.* **183**, 2632–2641
26. Blanchette, C.D., Woo, Y.H., Thomas, C., Shen, N., Sulchek, T.A., and Hiddessen, A.L. (2009) Decoupling internalization, acidification and phagosomal-endosomal/lysosomal fusion during phagocytosis of InlA coated beads in epithelial cells. *PLoS One* **4**, e6056
27. Katayama, H., Yamamoto, A., Mizushima, N., Yoshimori, T., and Miyawaki, A. (2008) GFP-like protein stably accumulate in lysosomes. *Cell Struct. Funct.* **33**, 1–12
28. Jahn, R. and Scheller, R.H. (2006) SNAREs—engines for membrane fusion. *Nat. Rev. Mol. Cell Biol.* **7**, 631–643

29. Nair-Gupta, P., Baccarini, A., Tung, N., Seyffer, F., Florey, O., Huang, Y., Banerjee, M., Overholtzer, M., Roche, P.A., Tampe, R., Brown, B.D., Amsen, D., Whiteheart, S.W., and Blander, J.M. (2014) TLR signals induce phagosomal MHC-I delivery from the endosomal recycling compartment to allow cross-presentation. *Cell* **158**, 506–521

Figure Legends

Figure 1.

Creation of *E. coli* probes expressing GST-tagged fluorescent proteins for the quantification of phagocytosis efficiency in J774 cells.

(A) Schematic representation of the GST-tagged fluorescent proteins expressed in *E. coli*. (B) Western blot showing the expression of GST-mCherry or GST-mCherry-mVenus in *E. coli* after induction with 1 mM IPTG. Proteins were detected using anti-GST-EGFP antibodies. (C) Fluorescence micrographs of J774 cells incubated with fixed and permeabilized *E. coli* probes expressing GST-mCherry (mCherry; upper panels). J774 cells were washed and fixed at the indicated time points. DIC: differential interference contrast. Scale bar: 10 μm. (D) Chart showing the efficiency of phagocytosis of *E. coli*-mCherry probes by J774 cells over time as described in *Materials and Methods*. The fluorescence ratio obtained at 60 min was defined as 1.0 in each experiment, and fluorescence, in arbitrary units, at other time points was normalized to this value. Data are presented as the mean ± SE of three independent experiments.

Figure 2.

***E. coli*-mCherry-mVenus is a useful, pH-sensitive probe that can be used to monitor changes in the phagosomal environment during the maturation process.**

(A) Chart showing the mVenus:mCherry fluorescence intensity (FI) ratio in buffers with decreasing pH. In each experiment, the FI ratio obtained with the *E. coli*-mCherry-mVenus probe in 25 mM Tris-HCl, pH7.0 was defined as 1.0, and all other measurements were normalized to this value. Data are presented as the mean ± SE of three independent experiments. (B) Chart showing the mVenus:mCherry FI ratio with increasing time following removal of the probe. J774 cells were incubated with fixed and permeabilized *E. coli*-mCherry-mVenus probes, unbound probe was removed, and FI was measured at the indicated time points (see *Materials and Methods* for details). The FI ratio obtained at 0 min was defined as 1.0 in each experiment, and other measurements were normalized accordingly. Data are presented as the mean ± SE of four independent experiments. (C) Fluorescence micrographs showing J774 cells treated with *E. coli*-mCherry-mVenus probes for 15 min on ice, followed by incubation for 30 min at 37°C. Excess probe was removed, and cells were incubated further for the indicated time periods before being fixed and analyzed by a confocal laser scanning microscopy. The wavelengths used to detect mCherry and mVenus are described in *Materials and Methods*. DIC: differential interference contrast. Scale bar: 10 μm.

Figure 3.

The *E. coli*-mCherry-mVenus probe is suitable for analysis of phagosome maturation processes, such as acidification and hydrolase activation.

(A) The mVenus:mCherry fluorescence intensity (FI) ratio after internalization of the *E. coli*-mCherry-mVenus probe by J774 cells and following treatment with the indicated concentrations of bafilomycin A1 (BafA1; open circles) or DPI (open triangles). The FI ratio was calculated as described in *Materials and Methods*. In each experiment, the FI ratio of untreated cells was defined as 1.0, and all other values were normalized to this value. Data are presented as the mean ± SE of three to five independent experiments. (B) Phagocytosis efficiency in the presence of the indicated concentration of BafA1 was estimated from the mCherry fluorescence values obtained in (A). For each experiment, the fluorescence obtained in the absence of BafA1 was taken to be 100%, and all other results were normalized to this value. Data are presented as the mean ± SE of five independent experiments. (C) Fluorescence micrographs of J774 cells incubated with *E. coli*-mCherry-mVenus probes in the presence or absence of 10 nM BafA1. The wavelengths used to detect mCherry and mVenus are described in *Materials and Methods*. DIC: differential interference contrast. Scale bar: 10 μm. (D) Western blot showing GST-mCherry-mVenus degradation products. Whole-cell extracts from J774 cells treated with the indicated concentrations of BafA1 were blotted, and the blots were probed with anti-RFP antibodies (α-RFP Ab) to detect degradation products. The broad, high-molecular-weight bands represent crosslinked GST-mCherry-mVenus probes. The major degradation product was approximately 28 kDa in size (dashed circle), and several other minor products were detected.

Figure 4.

Efficiency of the formation and maturation of phagosomes containing *E. coli* probes is enhanced in J774 cells overexpressing mVenus-SNAP-23.

J774 cells expressing mVenus (mV) or mVenus-SNAP-23 (mV-SNAP-23) were incubated with *E. coli*-mCherry-mVenus probes before fluorescence was measured as described in *Materials and Methods*. (A) The efficiency of association (left panel) and phagocytosis (right panel) of the probe with the indicated cell types as determined by mCherry fluorescence. In each experiment, the fluorescence signal obtained with control mV cells was defined as 100%, and the fluorescence obtained from mV-SNAP-23 cells was normalized to this value. Data are presented as the mean ± SE of six independent experiments. (B) Phagosome maturation efficiency of each cell type estimated from the mVenus:mCherry fluorescence intensity (FI) ratio. In each experiment, the FI ratio of the control mV cells was defined as 1.0, and the FI ratio of the mV-SNAP-23 cells was normalized to this value. Data are presented as the mean ± SE of six independent experiments.

An FI ratio <1.0 indicated enhanced phagosome maturation compared with control cells. (C) Western blot analysis of *E. coli*-mCherry-mVenus probe degradation after ingestion by mV or mV-SNAP-23 cells, in the presence or absence of 10 nM bafilomycin A1 (BafA1). Measurements at 0 h and 1 h represent samples taken immediately after incubation with the probe, following washing to remove unbound probe, and again 1 h later, respectively. Whole-cell extracts were probed using anti-RFP antibodies. The arrow indicates the 28 kDa degradation product in each experiment, and the dashed circle highlights the 28 kDa product in the absence of BafA1. BafA1 abolished the generation of this product. For each cell type, the level of the 28 kDa product observed at 0 h was defined as 1.00, and the size of the band after 1 h was normalized to this value (fold changes are shown below the panel).

Fig.1 Morita *et al*.

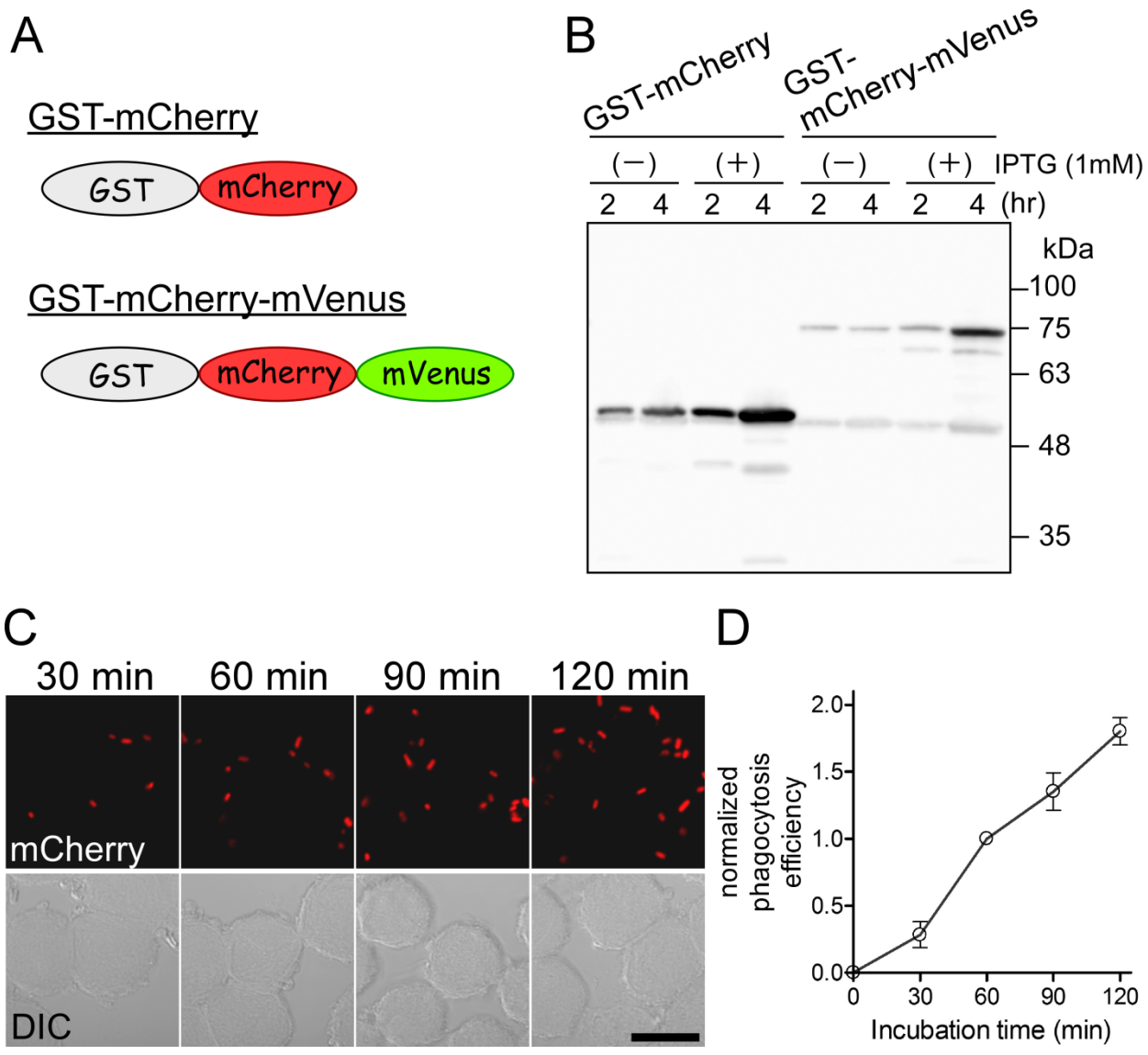

Fig.2 Morita *et al*.

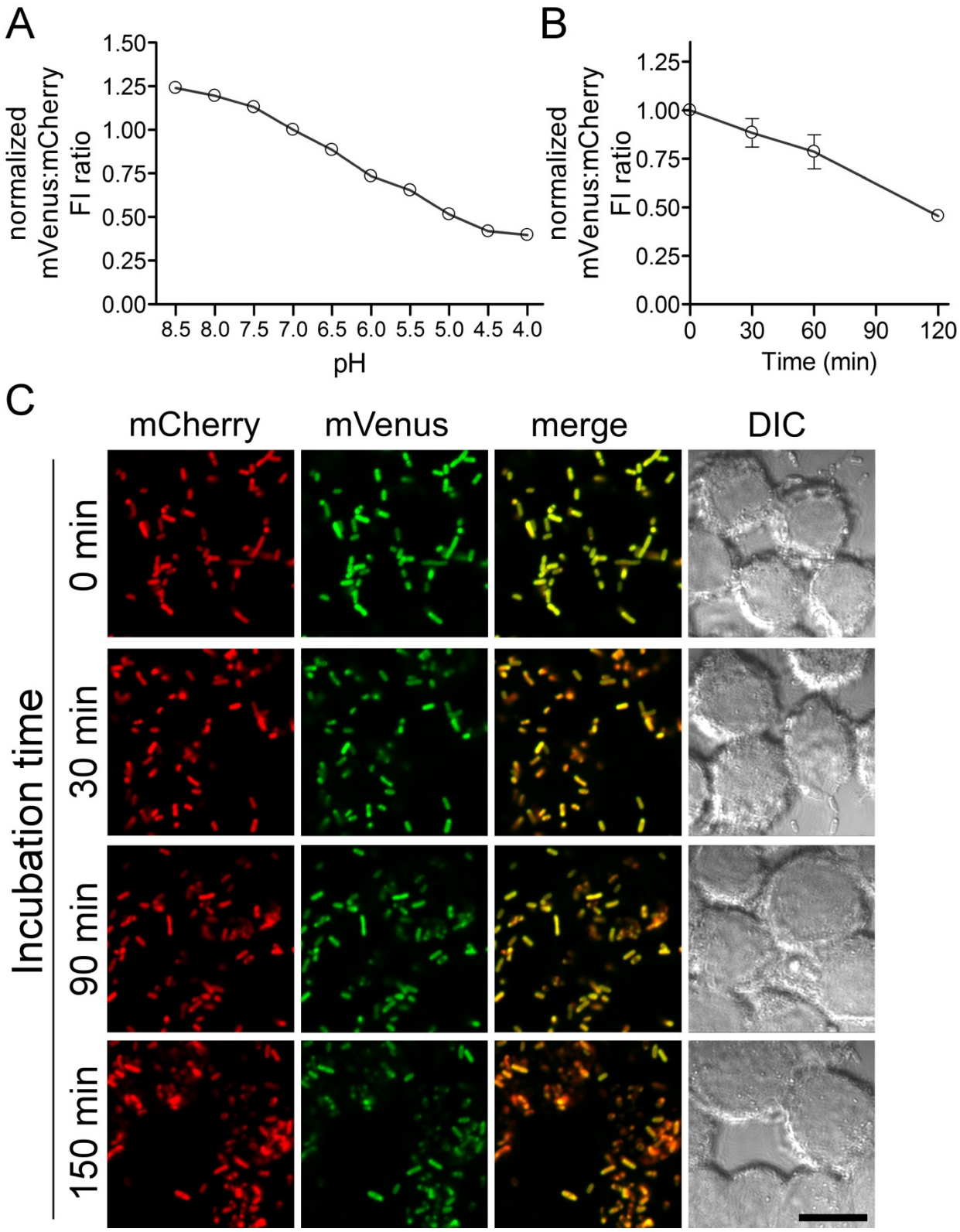

Fig.3 Morita *et al*.

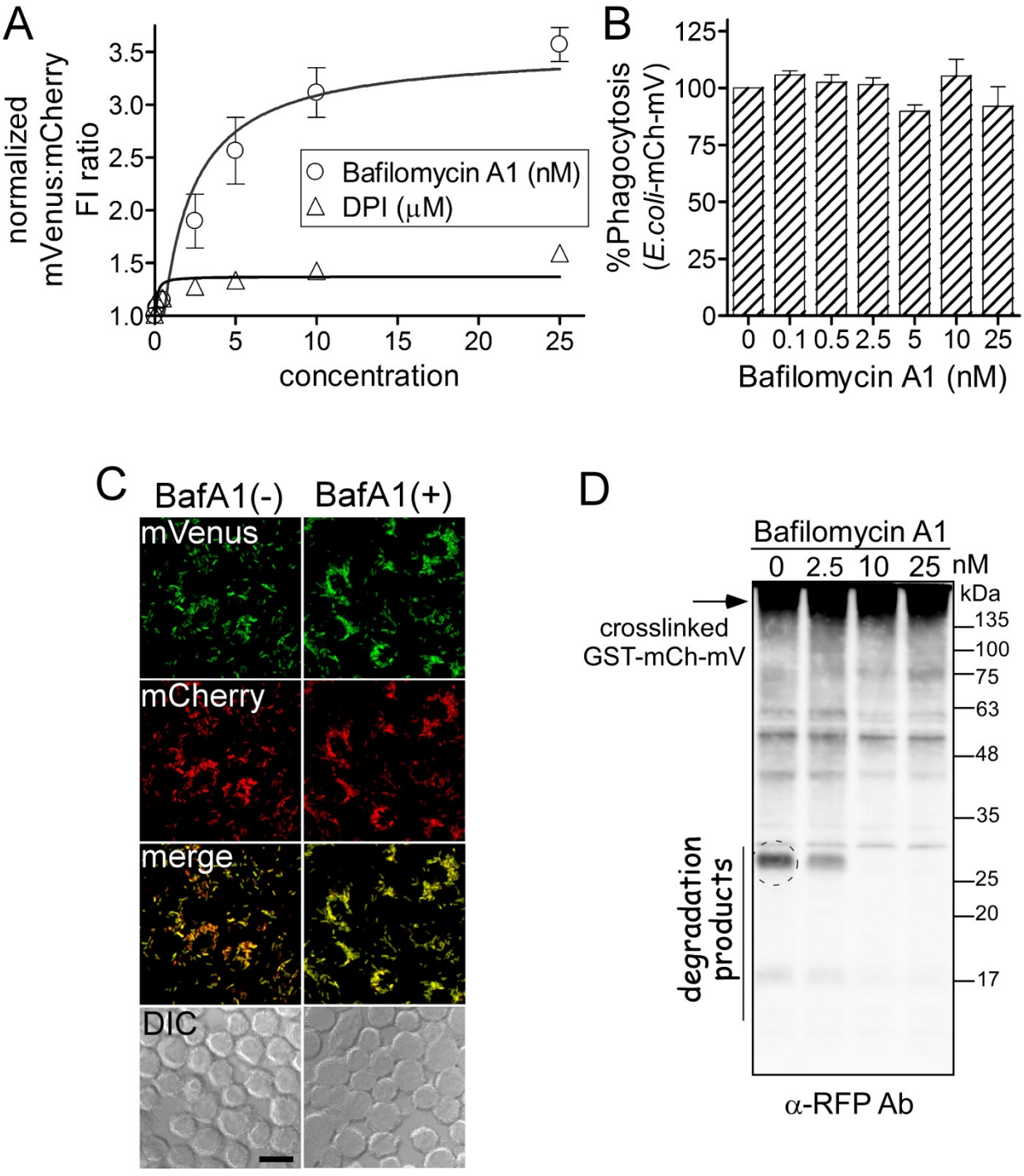

Fig.4 Morita *et al*.